Thermodynamics of Fusion Peptide−Membrane Interactions†

Yinling Li, Xing Han,‡ and Lukas K. Tamm*

Department of Molecular Physiology and Biological Physics, University of Virginia Health Sciences Center, P.O. Box 800736, Charlottesville, Virginia 22908-0736

Received January 31, 2003; Revised Manuscript Received April 8, 2003

ABSTRACT: The fusion peptides of viral membrane fusion proteins play a key role in the mechanism of viral spike glycoprotein mediated membrane fusion. These peptides insert into the lipid bilayers of cellular target membranes where they adopt mostly helical secondary structures. To better understand how membranes may be converted to high-energy intermediates during fusion, it is of interest to know how much energy, enthalpy and entropy, is provided by the insertion of fusion peptides into lipid bilayers. Here, we describe a detailed thermodynamic analysis of the binding of analogues of the influenza hemagglutinin fusion peptide of different lengths and amino acid compositions. In small unilamellar vesicles, the interaction of these peptides with lipid bilayers is driven by enthalpy (−16.5 kcal/mol) and opposed by entropy (−30 cal mol^{-1} K^{-1}). Most of the driving force ($\Delta G = -7.6$ kcal/mol) comes from the enthalpy of peptide insertion deep into the lipid bilayer. Enthalpic gains and entropic losses of peptide folding in the lipid bilayer cancel to a large extent and account for only about 40% of the total binding free energy. The major folding event occurs in the N-terminal segment of the fusion peptide. The C-terminal segment mainly serves to drive the N-terminus deep into the membrane. The fusion-defective mutations G1S, which causes hemifusion, and particularly G1V, which blocks fusion, have major structural and thermodynamic consequences on the insertion of fusion peptides into lipid bilayers. The magnitudes of the enthalpies and entropies of binding of these mutant peptides are reduced, their helix contents are reduced, but their energies of self-association at the membrane surface are increased compared to the wild-type fusion peptide.

Membrane fusion peptides play an important role in mediating fusion between two closely apposed membranes (see refs *1*−*4* for recent reviews). They are part of much larger fusion proteins, which are typically single-spanning integral membrane proteins with quite large ectodomains. In the resting (nonfusogenic) state, the hydrophobic fusion peptides are buried and protected in a hydrophobic crevice of the soluble ectodomain. After binding to an appropriate target membrane and triggering for fusion by an external stimulus (e.g., a drop in pH), the fusion proteins undergo a large conformational change, expel the fusion peptide from its protective crevice, and insert it into the target or host membrane, or both. This insertion of the fusion peptide into the lipid bilayer induces deformations of the membrane to the extent that it fuses with another membrane that has been brought into close proximity by the ectodomain. Even though this general principle of membrane fusion and the importance of the fusion peptide in this process have been recognized for quite some time (*5*−*8*), the mechanism of how fusion peptides exactly accomplish this task remains elusive.

Influenza virus enters cells by first binding to a cell surface receptor, followed by endocytosis and finally by a low-pH-induced fusion reaction. The fusion protein of influenza virus is the surface glycoprotein hemagglutinin (HA),[1] which harbors an ∼20-residue hydrophobic fusion peptide at the N-terminus of one of its two subunits. Using a fluorescence method, we have recently measured the binding of various HA fusion peptides to lipid bilayers (*9*). These studies yielded free energies of binding of these peptides at neutral pH and at the endosomal pH 5. To understand more deeply the thermodynamic underpinnings of the interaction of fusion peptides with lipid bilayers, we have now extended these studies by measuring the enthalpies of binding by high-sensitivity isothermal titration calorimetry (ITC).

ITC is an excellent technique to gain insight into the fundamental thermodynamic parameters that govern peptide binding to lipid bilayers (*10*). By titrating peptide to a large excess of lipid, one obtains the binding enthalpy, and by titrating lipid to peptide up to saturation, one obtains the free energy of binding. The entropy of binding can then be deduced from the familiar relation $\Delta G = \Delta H - T\Delta S$. Here, we have used peptide-to-lipid ITC titrations to determine ΔH and lipid-to-peptide fluorescence titrations to determine ΔG. Adding measurements of ΔH to those of ΔG allows us to ask whether fusion peptide binding is driven by enthalpy or entropy. If we also know the number of residues in α-helices in the membrane-bound forms of these peptides, we can

† Supported by National Institutes of Health Grant AI30557.

* Corresponding author. E-mail: lkt2e@virginia.edu. Phone: (434) 982-3578. Fax: (434) 982-1616.

‡ Current address: DuPont Haskell Laboratory for Health and Environmental Sciences, P.O. Box 50, Newark, DE 19714.

[1] Abbreviations: CD, circular dichroism; HA, hemagglutinin; HEPES, *N*-(2-hydroxyethyl)piperazine-*N*′-2-ethanesulfonic acid; ITC, isothermal titration calorimetry; LUV, large unilamellar vesicle; MES, 2-(4-morpholino)ethanesulfonic acid; NBD, 7-nitrobenz-2-oxa-1,3-diazole; POPC, 1-palmitoyl-2-oleoyl-3-*sn*-phosphatidylcholine; POPG, 1-palmitoyl-2-oleoyl-3-*sn*-phosphatidylglycerol; SUV, small unilamellar vesicle.

10.1021/bi0341760 CCC: $25.00
Published on Web 05/17/2003

further determine the respective relative contributions to ΔG, ΔH, and ΔS of folding and membrane insertion, using published per-residue values of ΔG, ΔH, and ΔS for folding of helical peptides in lipid bilayers.

The structure of the full-length fusion peptide in detergent micelles and lipid bilayers is characterized by two helices connected by a turn at around residue 12 (*11*). Therefore, the peptide forms a V-shape when it binds to bilayers with the apex at the interface and the N-terminal arm penetrating deep into one monolayer of the bilayer (*11*). To determine which parts of the fusion peptide sequence contribute most to the ΔG, ΔH, and ΔS of folding and insertion, we have carried out thermodynamic experiments at pH 5 for a series of HA fusion peptides of different lengths. Measuring the relevant thermodynamic parameters of fusion peptides of increasing lengths, we find that the N-terminal half is responsible for the largest increments in ΔG, ΔH, and ΔS. While ΔG is dominated by partitioning, folding contributes significantly to ΔH and dominates ΔS. In highly curved small unilamellar vesicles, binding of the fusion peptides is driven by ΔH and opposed by ΔS.

In a second group of experiments, we wanted to know how a small, but functionally important, perturbation at the N-terminus of the fusion peptide would affect the thermodynamic parameters of membrane interaction. It has been known for more than 20 years that the glycine in position 1 of the influenza HA fusion peptide is important for fusion (*12*). Rather small changes of the N-terminus can affect the structure of this fusion peptide and its interaction with membrane lipids (*13*). When this residue is replaced by a serine, fusion is arrested at the so-called hemifusion intermediate (*14*). In the hemifused state, two membranes are joined and lipid can flow freely between them, but a fusion pore, which allows exchange of aqueous contents between the two membrane-enclosed compartments, does not occur. However, when glycine-1 is replaced by a valine, fusion is completely blocked (*14*). Therefore, we synthesized analogues of the 20-residue fusion peptide with serine and valine replacements for glycine 1, i.e., the G1S and G1V mutant peptides. We measured the binding constants, secondary structures, and enthalpies of binding of these peptides and compared them to those of the wild-type peptide. The magnitudes of these three independent measures of lipid interaction all decreased in the order wild-type > G1S > G1V. The differences between G1S and G1V were larger than those between wild-type and G1S.

MATERIALS AND METHODS

Peptides and Lipids. All peptides were synthesized by solid-phase synthesis by the Biomolecular Research Facility at the University of Virginia using Fmoc chemistry. The C-termini were amidated. The peptides were purified by reverse-phase HPLC on a Vydac C4 column using a water/TFA−acetonitrile gradient solvent system. They were estimated to be >97% pure. Peptides were subjected to amino acid analysis to confirm their composition and to determine concentrations of stock solutions. All peptides showed single peaks of the expected relative molecular mass by MALDI mass spectrometry. Synthetic phospholipids were purchased from Avanti Polar Lipids (Alabaster, AL) and were used without further purification.

Preparation of Lipid Vesicles. A defined amount of lipid in chloroform was first dried under a nitrogen stream and subsequently overnight under high vacuum. Buffer (5 mM HEPES, 10 mM MES, pH 5) was added and vortexed to give a 5 mM lipid dispersion. The dispersion was then sonicated in an ice−water bath using a Branson titanium tip ultrasonicator until the solution became transparent (about 60 min at 50% duty cycle).

Isothermal Titration Calorimetry. All ITC measurements were carried out at 25 °C in a high-sensitivity MCS titration calorimeter (MicroCal Inc., Northampton, MA). All solutions were degassed for 20 min prior to use. For each injection, 10 μL of a 12−18 μM stock solution of peptide were injected into the sample cell which contained 2 mL of a 5 mM dispersion of small unilamellar vesicles composed of POPC:POPG (4:1). Data were analyzed utilizing Origin 6.0 and Grams/32.

CD Spectroscopy. For CD spectroscopy, 0.09 mM peptides were bound to 9 mM SUVs of POPC:POPG (4:1, mol/mol) in 5 mM HEPES and 10 mM MES, pH 5 (*9*). Spectra were recorded at 25 °C on a Jasco 600 spectropolarimeter as described previously. The fraction of residues in α-helical conformation, f_H, was estimated from the measured mean residue ellipticity at 222 nm, θ_{222}, by $f_H = (\theta_{222} - \theta_c)/(\theta_H - \theta_c)$, where $\theta_H = (250T - 44000)(1 - 3/n)$ and $\theta_c = 2220 - 53T$ are the limiting values of θ_{222} for completely helical and completely random coil peptides, respectively. T is the temperature in centigrade and n is the number of residues of the peptides (*15*, *16*).

Binding Experiments. Binding of NBD-labeled peptides to lipid bilayers was measured as previously described (*9*, *17*). POPC:POPG (4:1) SUVs were added successively to 0.05 μM fluorescent peptides in 5 mM HEPES and 10 mM MES, pH 5. Fluorescence intensities were measured with the excitation, emission, and slits set at 490, 530, and 5 nm, respectively. Light scattering was negligible under these conditions. The binding isotherms were fitted to a cooperative partition/self-association model as described in more detail in refs *17* and *18*. Briefly, binding is described by the partition equilibrium

$$X_b = K_{app} C_f \quad (1)$$

where K_{app} is the apparent partition coefficient in units of M^{-1}, X_b is the mol fraction of bound peptide per lipid, and C_f is the free peptide concentration. Plots of X_b vs C_f yield straight lines with a slope of K_{app} if a simple partition equilibrium is observed. However, if the peptides, in addition to partitioning, self-associate at the membrane surface, a cooperative binding model is adopted where K_{app} is replaced by σs. σ is the cooperativity parameter, and s is the equilibrium constant for the cooperative addition of further subunits after the nucleating insertion step. The binding equation then becomes

$$X_b = \sigma s \frac{C_f}{(1 - sC_f)^2} \quad (2)$$

Since our peptides are charged and interact with charged surfaces, we define the intrinsic partition coefficient

$$K_0 = \sigma s_0 = K_{app} \exp(z_p F \psi_0 / RT) = \sigma s \exp(z_p F \psi_0 / RT) \quad (3)$$

H7ac	CH_3CONH-GCGKKKK-$CONH_2$
P8H7	**GLFGAIAG**-GCGKKKK-$CONH_2$
P13H7	**GLFGAIAGFIENG**-GCGKKKK-$CONH_2$
P16H7	**GLFGAIAGFIENGWEG**-GCGKKKK-$CONH_2$
P20H7	**GLFGAIAGFIENGWEGMIDG**-GCGKKKK-$CONH_2$
G1S	**SLFGAIAGFIENGWEGMIDG**-GCGKKKK-$CONH_2$
G1V	**VLFGAIAGFIENGWEGMIDG**-GCGKKKK-$CONH_2$

FIGURE 1: Sequences of synthetic influenza hemagglutinin host−guest fusion peptides used in this study.

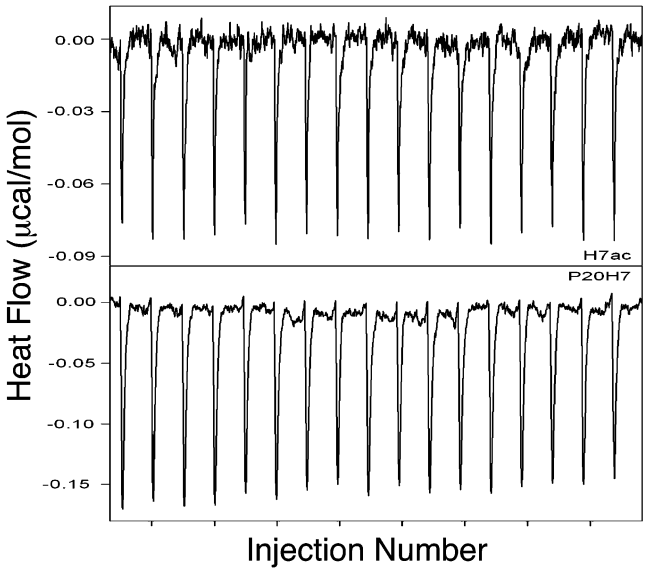

FIGURE 2: Calorimetric heat flows resulting from multiple injections of 10 μL aliquots of peptide to POPC:POPG (4:1) vesicles at 25 °C. Top: H7ac host peptide. Bottom: P20H7 fusion peptide.

where z_p is the net charge of the peptide, ψ_0 is the surface potential, and F is Faraday's constant. In symmetric electrolytes, ψ_0 is determined from the Gouy−Chapman equation (*19*)

$$\sinh(ze\psi_0/2kT) = A\sigma/(c)^{1/2} \quad (4)$$

A is a constant equal to $(8\epsilon_r\epsilon_0 kT)^{-1/2}$, σ is the surface charge density, and c is the number of ions of charge z per liter of a z:z electrolyte in the bulk aqueous solution. All other symbols have their usual meanings. Having determined K_0, we find the free energy of insertion

$$\Delta G_{ins} = -RT \ln(55.5K_0) \quad (5)$$

RESULTS

The sequences of the peptides used in this study are shown in Figure 1. They represent different lengths, namely 8, 13, 16, and 20 residues, of the influenza hemagglutinin fusion peptide sequence coupled to a polar peptide at the C-terminus to render the peptides more water soluble. In this host−guest fusion peptide design, the polar C-terminal segments serve as surrogate polar ectodomains of HA that can also bind electrostatically to negatively charged lipid bilayers and thereby facilitate the unidirectional insertion of the peptides into membranes (*9*). All peptides are amidated at the C-terminus. The polar N-terminally acetylated host peptide, H7ac, was also synthesized in order to compare and subtract contributions of this moiety to the binding data.

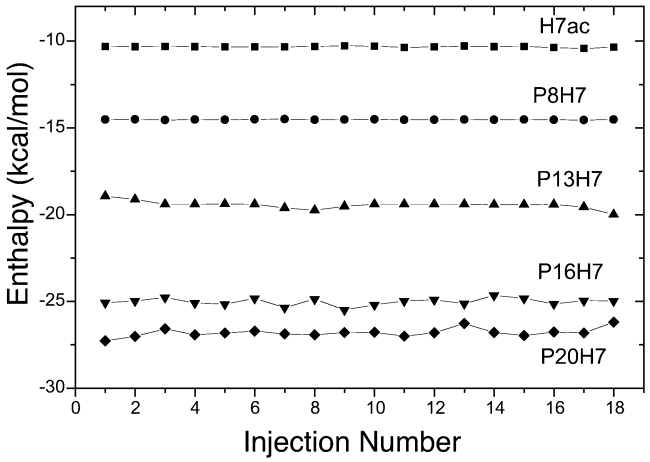

FIGURE 3: Reaction enthalpies of peptide binding to POPC:POPG (4:1) vesicles determined from the integration of calorimetric heat flow curves at 25 °C.

Table 1: Free Energy, Enthalpy, and Entropy of HA Fusion Peptide Binding to Lipid Bilayers at 298 K

peptide	ΔG (kcal/mol)	ΔH (kcal/mol)	ΔS (cal mol^{-1} K^{-1})	$-T\Delta S$ (kcal/mol)
H7ac	-0.89 ± 0.04[a]	-10.33 ± 0.10	-31.68	9.44
P8H7	-1.12 ± 1.17[a]	-14.53 ± 0.03	-45.00	13.41
P13H7	-3.57 ± 0.10[a]	-19.45 ± 0.55	-53.29	15.88
P16H7	-6.00 ± 0.16[a]	-25.02 ± 0.47	-63.83	19.02
P20H7	-8.50 ± 0.99[a]	-26.80 ± 0.60	-61.41	18.30
G1S	-7.70 ± 0.12	-26.27 ± 0.84	-62.32	18.57
G1V	-6.66 ± 0.27	-19.50 ± 0.47	-43.09	12.84

[a] From ref *9*.

To measure enthalpies of fusion peptide binding to lipid bilayers, we injected small aliquots of a concentrated peptide stock solution into a large volume of pH 5 buffer containing small unilamellar vesicles composed of POPC and POPG (4:1, mol/mol) and measured the associated heat flows in an isothermal titration calorimeter. Each addition gave rise to a transient decrease of the heat flow in the sample relative to the reference cell, indicating an exothermic reaction (Figure 2). Part of the dissipated heat is due to the heat of mixing, another part to the interaction of the H7 segment with the lipid bilayers, and a third part to the interaction of the fusion peptide segment with the lipid bilayers. The first two parts were measured separately with the H7ac peptide (top panel of Figure 2). Integration of these peaks yielded a contribution of -10.3 ± 0.1 kcal/mol (Figure 3). The lower panel of Figure 2 shows the calorimetric heat flows after several additions of the full-length fusion peptide P20H7. Integration of these peaks leads to a reaction enthalpy of -26.8 ± 0.6 kcal/mol. Similar data for the shorter fusion peptides can be found in Figure 3, and the resulting averaged reaction enthalpies are listed in Table 1. Subtracting the H7 contribution from P20H7 yields a binding enthalpy of -16.5 kcal/mol for the 20-residue fusion peptide. This value and corresponding numbers for the shorter fusion peptides are listed in Table 2. The negative (exothermic) binding enthalpies increase substantially with each increment of residues up to 16 residues and then to a lesser degree when the peptide is further elongated to 20 residues. This is graphically shown in Figure 4. The larger contribution of the N-terminal residues compared to the C-terminal residues of the fusion peptide to the binding enthalpy is not surprising because the

Table 2: Difference Thermodynamic Parameters $\Delta\Delta G$, $\Delta\Delta H$, and $\Delta\Delta S$ of HA Fusion Peptide Binding to Lipid Bilayers at 298 K

peptide	$\Delta\Delta G$ (kcal/mol)	$\Delta\Delta H$ (kcal/mol)	$\Delta\Delta S$ (cal mol^{-1} K^{-1})	$-T\Delta\Delta S$ (kcal/mol)	no. of helical residues in membrane-bound form
H7ac	0	0	0	0	0[a]
P8H7	−0.2	−4.2	−13.3	4.0	0[a]
P13H7	−2.7	−9.1	−21.6	6.4	6.5[a]
P16H7	−5.1	−14.7	−32.2	9.6	11.5[a]
P20H7	−7.6	−16.5	−29.7	8.9	13[a]
G1S	−6.8	−15.9	−30.6	9.1	11
G1V	−5.8	−9.2	−11.4	3.4	7

[a] From ref *9*.

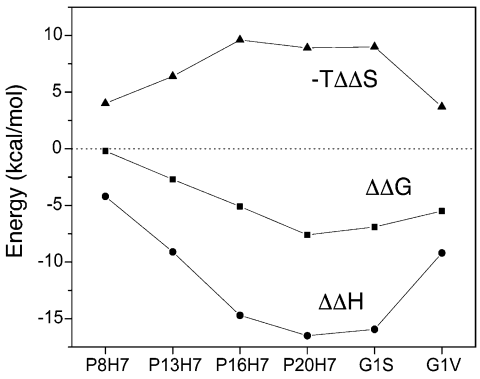

FIGURE 4: Free energies, enthalpies, and entropies of peptide binding to POPC:POPG (4:1) vesicles at 25 °C. Entropies were converted into energy units by multiplication with −298 K.

N-terminal half is more hydrophobic and inserts more deeply into the membrane than the C-terminal half of the HA fusion peptide (*11*).

The free energies of binding of this same series of peptides have been determined previously by quantitative measurements of partitioning of the peptides to small unilamellar vesicles of POPC and POPG (4:1) (*9*). More recently, we confirmed the spectroscopically determined ΔG's of the NBD-labeled peptides by performing ITC titrations of lipid vesicles to unlabeled peptides (L. Lai and L. K. Tamm, unpublished results). Since both methods yielded essentially the same results, we conclude that the label had no significant effect on the measured values. Entropies of binding were then calculated for each peptide from $\Delta G = \Delta H - T\Delta S$. The earlier free energy data and the newly determined entropies of binding are also listed in Tables 1 and 2 and plotted in Figure 4. The entropies of binding are also negative, and their magnitudes increase almost linearly up to P16H7 and then remain approximately constant for the last four-residue increment of P20. When converted into energy units by multiplication with −298 K, the entropic contribution to the free energy becomes positive, i.e., opposes binding of all peptides. The balance of enthalpy and entropy, i.e., the free energy, is still negative, and the total binding strength increases almost linearly as the fusion peptide is elongated all the way to its full length (Figure 4). At all lengths, peptide association with the lipid bilayers is driven by enthalpy and not entropy.

Previous fusion studies have shown that the first residue of the fusion peptide is extremely critical for its activity (*14*). Replacing this glycine with a serine leads to hemifusion (i.e., mixing of lipids but not aqueous compartment contents), and substitution with a valine blocks fusion completely. Therefore, we were interested to find out whether these substitutions would also lead to structural changes of the corresponding fusion peptides in lipid bilayers and whether the thermodynamics of membrane binding were perturbed by these changes. Host−guest peptides with the G1S and G1V substitutions were synthesized (Figure 1). Figure 5 shows the binding (partitioning) of these peptides to SUVs of POPC:POPG (4:1) in comparison to the wild-type peptide. While the wild-type peptide exhibited a simple partition equilibrium that was characterized by a straight line, the binding of both mutant peptides was initially depressed but then increased at high concentrations. This behavior is typical for cooperative binding coupled with self-association of fusion peptides at the membrane surface as discussed in detail in Han and Tamm (*17*). Using the partition/self-association model described in that earlier work, we determined free energies of insertion and the free energies of self-association for each of the peptides (Table 3). It is clear from this analysis that the magnitude of the free energy of insertion decreased by 0.8 kcal/mol for the G1S mutant and by 1.8 kcal/mol for the G1V mutant. G1S and G1V exhibited free energies of self-association at the membrane surface of −2.3 and −3.5 kcal/mol, respectively.

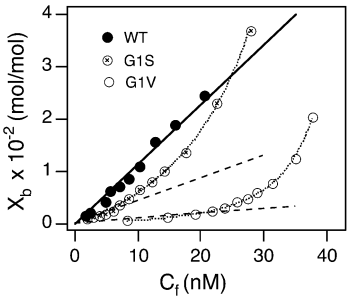

FIGURE 5: Binding of P20H7 (wild-type), G1S, and G1V fusion peptides to lipid bilayers composed of POPC:POPG (4:1) shown as plots of moles of bound peptide per moles of lipid in the outer leaflet of the vesicles (X_b) vs the equilibrium concentration of free peptide in solution (C_f). The binding isotherms, recorded at 25 °C and pH 5, were fitted to a cooperative partition/self-association model (dotted lines) or approximated by a simple partition model (solid and dashed lines).

CD spectra of these peptides in SUVs of POPC:POPG (4:1) were recorded and compared to the spectrum of the wild-type peptide (Figure 6). These spectra all show two minima at about 208 and 222 nm, which is typical for α-helical secondary structures. Percents of residues in helical secondary structure were calculated for each of these peptides as described in Materials and Methods and found to be 48% for wild-type (*9*), 41% for the G1S, and 27% for the G1V mutants of P20H7. Apparently, the G1S substitution does not affect much the α-helical character of the influenza fusion peptide, but the G1V mutation more significantly decreases its helical content.

We also measured the enthalpy of binding of the G1S and G1V mutant peptides to lipid bilayers of POPC:POPG (4:1). These measurements were obtained under conditions of a large excess of lipid, where self-association of the peptides at the membrane surface was negligible and binding was dominated by peptide partitioning into the bilayer. As Figure 4 and Tables 1 and 2 show, the enthalpy of membrane

Table 3: Thermodynamic Analysis of the Insertion and Self-Association of Wild-Type and Mutant HA Fusion Peptides in Lipid Bilayers at pH 5[a,b]

peptide	σ	s (M^{-1})	K_{app} (M^{-1})	K_0 (M^{-1})	ΔG_{ins}[c] (kcal/mol)	ΔG_{assoc}[c] (kcal/mol)
P20H7	1	1.3×10^6	1.3×10^6	3.1×10^4	-8.50 ± 0.99	0
G1S	2.1×10^{-2}	1.6×10^7	3.4×10^5	8.1×10^3	-7.70 ± 0.12	-2.29 ± 0.09
G1V	3.1×10^{-3}	2.0×10^7	6.2×10^4	1.5×10^3	-6.66 ± 0.27	-3.46 ± 0.28

[a] Derived from the data of Figure 5 using the binding model described in Materials and Methods. A surface potential of −96.1 mV was calculated from eq 4 and used for fitting eqs 2 and 3. [b] Average of three experiments. [c] $\Delta G_{ins} = -RT \ln(55.5K_0)$ and $\Delta G_{assoc} = +RT \ln \sigma$.

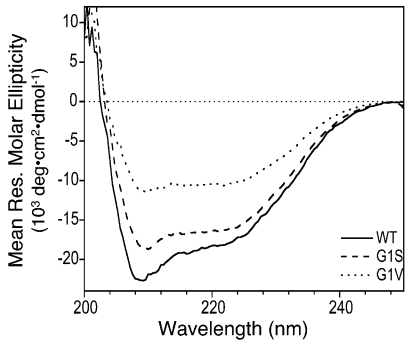

FIGURE 6: CD spectra of P20H7 (solid line), G1S (dashed line), and G1V (dotted line) fusion peptides bound to POPC:POPG (4:1) vesicles at pH 5.

insertion of G1S was only 0.6 kcal/mol smaller than that of the wild-type fusion peptide, but the enthalpy of membrane insertion of G1V was 7.3 kcal/mol smaller than that of the wild-type peptide. The entropy of insertion was also not much changed for G1S but was significantly reduced for G1V.

Membrane binding and insertion of all except the shortest of these fusion peptides are accompanied by folding into an α-helix (*9*). Therefore, the question arises as to what fractions of the measured energies and entropies are due to folding and what fractions are due to insertion into the lipid bilayer. Wieprecht et al. (*20*) measured the relevant per-residue thermodynamic parameters for the coil → helix transition in a membrane environment for the case of the amphipathic peptide magainin. They determined the enthalpy change of folding to be −0.7 kcal/mol per residue, the entropy change of folding to be −1.9 cal mol^{-1} K^{-1} per residue, and the free energy change of folding to be −0.14 kcal/mol per residue in small unilamellar vesicles. Similar values were later confirmed in large unilamellar vesicles (*21*). Ladhokin and White measured a free energy change of −0.4 kcal/mol per residue for the folding of mellitin in membranes (*22*). Our own best estimate of this value is -0.25 ± 0.05 kcal/mol per residue.[2] We calculated the contribution of folding

[2] A linear regression of the thermodynamic data vs the number of helical residues in Table 2 yields per-residue values of −0.53 kcal/mol, −1.0 kcal/mol, and −1.6 cal mol^{-1} K^{-1} for ΔG, ΔH, and ΔS, respectively. However, these values must be overestimates of folding because insertion is also expected to increase as the length of the peptides is increased. If we only use peptides P20H7, G1S, and G1V, which all have the same length and therefore should have similar values of insertion, we obtain a ΔG of folding of −0.29 kcal/mol per residue, which is midway between the previously reported extremes of −0.14 kcal/mol (*20*) and −0.4 kcal/mol (*22*). Because of small insertion differences between the three peptides our value may still be a slight overestimate. Therefore, we believe the true value is in the range -0.25 ± 0.05 kcal/mol per residue. Since similar estimates of ΔH and ΔS of folding are relatively close to the published values (*20*), we used the latter in our calculations.

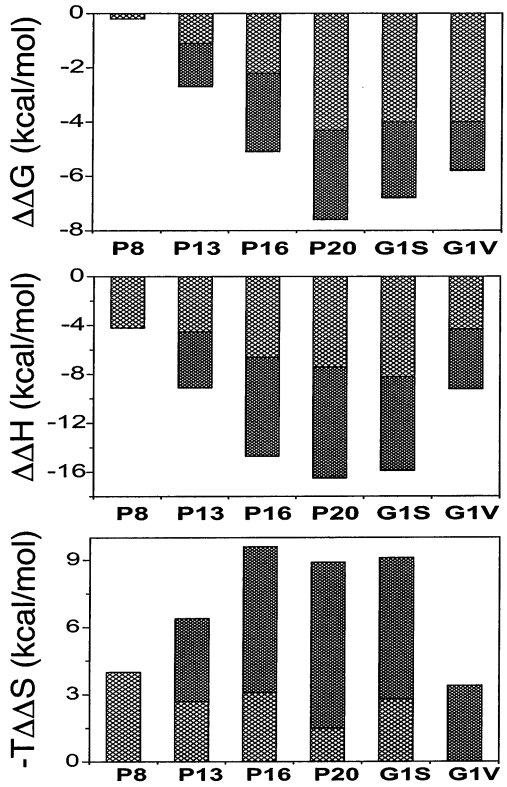

FIGURE 7: Contributions of membrane insertion and folding to the thermodynamics of fusion peptide binding to lipid bilayers. The lighter hatched areas represent contributions from insertion, and the darker hatched areas represent contributions from folding.

to the total membrane interaction energy for each of our peptides using the known fractions of α-helix (Table 2) and -0.25 ± 0.05 kcal/mol, −0.7 kcal/mol, and −1.9 cal mol^{-1} K^{-1} per folded residue for ΔG, ΔH, and ΔS, respectively. These results are graphically presented in Figure 7. If we consider only the free energies, it is evident that 55−70% of the interaction energy comes from insertion and the rest from folding for the full-length fusion peptides. The ΔG's of shorter peptides are made up of about 60% folding and 40% insertion. However, when enthalpies and entropies are considered separately, we find that, except for the shortest peptide, which does not fold, the enthalpy contributions are split about 50:50 between folding and insertion and that the entropy contributions to folding clearly dominate over those of insertion. Obviously, a large enthalpy−entropy compensation of the folding contributions mitigates their effect on ΔG so that the free energies of the full-length peptides are dominated by insertion rather than folding.

DISCUSSION

The studies presented here provide a first comprehensive thermodynamic analysis of the binding of fusion peptides

to lipid bilayers. The main results are (i) that the thermodynamic parameters increase almost linearly as the peptide is elongated and inserts more deeply into the membrane, (ii) that binding to highly curved SUVs is driven by enthalpy and opposed by entropy, (iii) that most of the free energy gain is due to peptide insertion, but most of the entropic cost is due to peptide folding in the membrane, and (iv) that small perturbations of the N-terminal glycine, which alter the fusion behavior of influenza hemagglutinin, have quite dramatic effects on the thermodynamics of fusion peptide−lipid interactions. These four results will be discussed in the following separate sections.

Thermodynamic Consequences of "Growing" the Fusion Peptide into Lipid Bilayers. The structure of the influenza HA fusion peptide has been determined in dodecylphosphocholine micelles by NMR and in lipid bilayers by site-directed spin-label EPR spectroscopy (*11*). Residues 1−10 form a helix that inserts into the membrane at an angle of about 37° from the membrane surface. The N-terminus therefore reaches about 10−15 Å into the outer leaflet of the bilayer. The more deeply embedded face of this helix contains mostly bulky hydrophobic residues, whereas the surface-exposed face contains a ridge of glycines. Residues 11−13 form a turn, and residues 14−18 form a short 3_{10}-helix, which inserts at the interface of the lipid bilayer. Although the NMR and EPR structures of the shorter fusion peptide analogues have not been determined, their secondary structures and approximate disposition in the membrane are known from CD and polarized FTIR studies (*9*, *17*). These and the full-length peptides are predominantly unstructured in solution but helical when inserted into lipid bilayers (*9*).

The entropy cost of restricting the mobility of the unstructured P8H7 to the membrane surface is −13.3 cal mol^{-1} K^{-1} (Table 2). Six to seven residues fold into a helix when P13H7 binds to lipid bilayers. Binding yields −2.7 kcal/mol in free energy and −9.1 kcal/mol in enthalpy but costs 6.4 kcal/mol in entropy. Elongating the helix with three more residues (P16H7) induces folding of five more residues and results in additional free energy and entropy gains of −2.4 and −5.6 kcal/mol, respectively, and an additional entropy cost of 3.2 kcal/mol. Only one or two more residues fold into a helix when P16H7 is extended to P20H7. This is consistent with the NMR structure, which is more helical in the N-terminal than in the C-terminal half of the molecule. Accordingly, only a small enthalpy gain and practically no entropy loss occur upon this C-terminal extension. The extension allows the small 3_{10}-helix (which may be rather dynamic) to form and pushes the more stable N-terminal helix deeper into the membrane. The small increment in ΔH and the essentially unchanged ΔS are also consistent with the general result (discussed below) that peptide *folding* is associated with large enthalpy and entropy changes but that peptide *insertion* into highly curved bilayers is mainly driven by enthalpy with only a small entropy change.

The sequence of thermodynamic events as a result of peptide elongation not only is of basic interest for our understanding of the energetics of peptide−lipid interactions, but may have functional and temporal counterparts in the physiological fusion reaction. A coupled insertion−folding process likely occurs in fusion when the fusion peptide reaches the target membrane. Folding of the 10-residue N-terminal helix is only induced after all residues of this helix have reached the membrane surface. Elongation up to residue 16 induces further enthalpy-driven folding and insertion. Further extension to residue 20 is accompanied with the formation of the amphipathic 3_{10}-helix (residues 14−18), which pushes the N-terminus deeper into the membrane. The resulting angled and deeply inserted N-terminal helix seems to be required for fusion (*9*, *23*).

Binding of Fusion Peptides to SUVs Is Driven by Enthalpy and Opposed by Entropy. A striking result of this work is that the binding of all peptides studied here is driven by large enthalpy gains. The associated entropy change does *not* favor binding. This finding is opposed to the common belief that binding of such peptides is driven by the (classical) hydrophobic effect, which has its origin in the *gain* of entropy when water molecules are displaced from two combining hydrophobic surfaces (*24*). The so-called nonclassical enthalpy-driven hydrophobic effect has been described before for the binding of several other peptides to SUVs (*10*, *25*). It has been explained by attractive van der Waals forces between the peptide and lipid bilayer. In our analysis, the electrostatic contributions to the binding have been eliminated by applying the Gouy−Chapman theory, which accounts for excess peptide concentrations near the membrane surface due to electrostatic attraction/repulsion. In addition, the contributions of the polar C-terminal carrier peptide (H7) were eliminated by subtracting the appropriate terms from the measured thermodynamic values. Therefore, the reported values refer to the nonpolar interactions of the fusion peptide proper.

Recent studies have shown that the domination of peptide binding by enthalpy may be limited to the highly curved membranes of SUVs, as this effect is much less pronounced when measured in more planar LUVs (*21*). Although the values of ΔG are not much affected by curvature, the relative contributions of ΔH and ΔS are. The origin of this energy−entropy compensation is not clear, but the larger energetic contributions in SUVs compared to LUVs have been explained by increased curvature strain that is stored in SUVs and that can be released upon peptide binding (*10*). Since viral membrane fusion is believed to be promoted by highly curved intermediate lipid structures, it is not a priori clear whether SUVs or LUVs would be the better (more physiological) model system for binding studies as reported here. Regardless, it has been shown before for two different peptide systems that only the insertion but not folding contributions to ΔH and ΔS are affected by membrane curvature (*21*, *26*).

Contributions of Folding and Insertion to the Energetics of Fusion Peptide Binding. Binding of all except the shortest peptide of this study is accompanied by a random coil → helix transition (*9*). Therefore, a fraction of the changes in ΔG, ΔH, and ΔS must be due to folding, and another fraction arises from insertion. Two laboratories have recently measured the folding contributions to ΔG and found quite different values, namely, −0.14 kcal/mol per residue (*20*) and −0.4 kcal/mol per residue (*22*). The origin of this difference is not quite clear. It is not due to different vesicle sizes (*21*) but could be due to the different immersion depths of the peptides or to experimental differences between the two studies. Our own results indicate that this value is in the range -0.25 ± 0.05 kcal/mol.[2] Helix formation of homo-

polymers in water is accompanied with a ΔG of −0.08 to −0.11 kcal/mol per residue at 25 °C (*27*). All three values thus far determined in membranes are *larger*. The ΔH and ΔS of folding of homopolymers and a model peptide in water are −0.9 to −1.3 kcal/mol (*27*−*30*) and −2.7 to −3.4 cal mol^{-1} K^{-1} (*27*) per residue, respectively. In membranes these values are *smaller*, i.e., −0.5 to −0.8 kcal/mol and −1.0 to −2.3 cal mol^{-1} K^{-1} per residue, respectively (*20*, *21*, *26*). A similar value of ΔH (−0.7 kcal/mol per residue) has been reported for folding in the less polar environment of trifluoroethanol/water (*16*). Applied to our full-length fusion peptides, we find that folding contributes about 44% or less to the total ΔG of binding (Figure 7). This is less than what has been reported for magainin (∼50%) and melittin (∼66%) (*20*, *22*). However, compared to these other peptides, the fusion peptides are less helical, yet penetrate deeply into the membrane (*11*, *23*). Folding of the fusion peptides contributes ≥50% to ΔH and 60−100% to ΔS, which is similar to the values reported for magainin ($\Delta H_{fold} \approx 72\%$; $\Delta S_{fold} \approx 82\%$) and a mitochondrial presequence ($\Delta H_{fold} \approx 56\%$; $\Delta S_{fold} \approx 56\%$) (*20*, *21*, *26*).

Effect of Perturbation of the N-Terminus of the HA Fusion Peptide: G1S and G1V Mutants. Replacing the C-terminal and highly conserved glycine residue of the influenza HA fusion peptide with a serine or a valine has a dramatic effect on the structure of this peptide in DPC micelles (X. Han and L. K. Tamm, unpublished results). These structural changes are also reflected in the CD spectra of these peptides in lipid bilayers (Figure 6). While the wild-type peptide comprises about 13 helical residues in membranes, G1S and G1V have about 11 and 7 helical residues, respectively (Table 2). In the context of the full-length HA, the G1S mutation causes hemifusion and the G1V mutation blocks fusion altogether (*14*). Therefore, the stage to which fusion can proceed correlates with the amount of helicity of these three peptides.

The data presented in Figures 4 and 5 and Tables 1−3 establish that the energetics of fusion peptide binding also correlate with fusion activity. The enthalpies and entropies are much more affected than the free energies of binding, especially when G1V and the wild-type peptide are compared. As was seen with the peptides of different lengths, enthalpy and entropy cancel to some extent to mitigate the effects of the mutations on the free energies. Therefore, enthalpy measurements may be better than measurements of free energy to distinguish between peptides that cause and peptides that do not cause fusion.

Another dramatic difference between the wild-type and mutant fusion peptides is the much higher tendency of the mutants, especially the G1V mutant peptide, to self-associate at the membrane surface at high concentrations (Figure 5). While the wild-type peptide did not self-associate at low ionic strength, G1S and G1V exhibited free energies of self-association of −2.3 and −3.5 kcal/mol, respectively (Table 3). FTIR spectra show that self-association of these peptides at the membrane surface is accompanied by a helix → β-sheet transition (X. Han and L. K. Tamm, unpublished results; see also ref *17*). Therefore, forming too much β-sheet by fusion peptide self-association in membranes seems to be detrimental to their fusion activity. We conclude that fusion is promoted by the deep insertion of the fusion peptide into lipid bilayers and its concomitant folding into a kinked α-helical structure. Both processes are driven by enthalpy in highly curved lipid bilayers.

REFERENCES

1. Durell, S. R., Martin, I., Ruysschaert, J. M., Shai, Y., and Blumenthal, R. (1997) *Mol. Membr. Biol. 14*, 97−112.
2. Pécheur, E. I., Sainte-Marie, J., Bienvenüe, A., and Hoekstra, D. (1999) *J. Membr. Biol. 167*, 1−17.
3. Martin, I., and Ruysschaert, J. M. (2000) *Biosci. Rep. 20*, 483−500.
4. Tamm, L. K., and Han, X. (2000) *Biosci. Rep. 20*, 501−518.
5. Gething, M. J., Doms, R. W., York K., and White J. (1986) *J. Cell Biol. 102*, 11−23.
6. Murata, M., Sugahara, Y., and Ohnishi, S. I. (1987) *J. Biochem. 102*, 957−962.
7. Lear, J. D., and DeGrado, W. F. (1987) *J. Biol. Chem. 262*, 6500−6505.
8. Wharton, S. A., Martin, S. R., Ruigrok, R. W. H., Skehel, J. J., and Wiley, D. C. (1988) *J. Gen. Virol. 69*, 1847−1857.
9. Han, X., and Tamm, L. K. (2000) *Proc. Natl. Acad. Sci. U.S.A. 97*, 13097−13102.
10. Seelig, J. (2002) in *Current Topics in Membranes, Vol. 52*: *Peptide−Lipid Interactions* (Simon, S. A., and McIntosh, T. J., Eds.) pp 31−56, Academic Press, New York.
11. Han, X., Bushweller, J. H., Cafiso, D. S., and Tamm, L. K. (2001) *Nat. Struct. Biol. 8*, 715−720.
12. Garten, W., Bosch, F. X., Linder, D., Rott, R., and Klenk, H. D. (1981) *Virology 115*, 361−374.
13. Gray, C., Tatulian, S. A., Wharton, S. A., and Tamm L. K. (1996) *Biophys. J. 70*, 2275−2286.
14. Qiao, H., Armstrong, R. T., Melikyan, G. B., Cohen, F. S., and White, J. M. (1999) *Mol. Biol. Cell 10*, 2759−2769.
15. Rohl, C. A., and Baldwin, R. L. (1997) *Biochemistry 36*, 8435−8442.
16. Luo, P., and Baldwin, R. L. (1997) *Biochemistry 36*, 8413−8421.
17. Han, X., and Tamm, L. K. (2000) *J. Mol. Biol. 304*, 953−965.
18. Spuhler, P., Anantharamaiah, G. M., Segrest, J. P., and Seelig, J. (1994) *J. Biol. Chem. 269*, 23904−23910.
19. McLaughlin, S. (1989) *Annu. Rev. Biophys. Biophys. Chem. 18*, 113−136.
20. Wieprecht, T., Apostolov, O., Beyermann, M., and Seelig, J. (1999) *J. Mol. Biol. 294*, 785−794.
21. Wieprecht, T., Beyermann, M., and Seelig, J. (2002) *Biophys. Chem. 96*, 191−201.
22. Ladokhin, A. S., and White, S. H. (1999) *J. Mol. Biol. 285*, 1363−1369.
23. Tamm, L. K. (2003) *Biochim. Biophys. Acta* (in press).
24. Tanford, F. (1980) *The Hydrophobic Effect*: *Formation of Micelles and Biological Membranes*, Wiley, New York.
25. Seelig, J., and Ganz, P. (1991) *Biochemistry 30*, 9354−9359.
26. Wieprecht, T., Apostolov, O., Beyermann, M., and Seelig, J. (2000) *Biochemistry 39*, 15297−15305.
27. Hermans, J. (1966) *J. Phys. Chem. 70*, 510−515.
28. Rialdi, G., and Hermans, J. (1966) *J. Am. Chem. Soc. 88*, 5719−5720.
29. Chou, P. Y., and Scheraga, H. A. (1971) *Biopolymers 10*, 657−680.
30. Scholtz, J. M., Marqusee, S., Baldwin, R. L., York, E. J., Stewart, J. M., Santoro, M., and Bolen, D. W. (1991) *Proc. Natl. Acad. Sci. U.S.A. 88*, 2854−2858.

BI0341760